Solar Energy Materials and Solar Cells 173 (2017) 12–17

Contents lists available at ScienceDirect

Solar Energy Materials and Solar Cells

journal homepage: www.elsevier.com/locate/solmat

Multiple pathways for permanent deactivation of boron-oxygen defects in p-type silicon

Nitin Nampalli*, Hongzhao Li, Moonyong Kim, Bruno Stefani, Stuart Wenham, Brett Hallam, Malcolm Abbott

School of Photovoltaic and Renewable Energy Engineering, University of New South Wales, Sydney, NSW 2052, Australia

ARTICLE INFO

Keywords:
Boron-oxygen defect
Silicon
Thermal deactivation
Thermal activation
Regeneration
Hydrogen
Passivation
Carrier lifetime
Rapid thermal annealing
Belt firing

ABSTRACT

In this work, it is shown that there are at least two separate pathways for the permanent deactivation of boron-oxygen defects – a purely thermal pathway involving the dissociation of defect precursors, and another mechanism based on passivation of the fully-formed defect during an illuminated annealing process (regeneration). Based on investigations on fired and non-fired p-type Czochralski silicon wafers, a thermal reduction in the net concentration of BO defects is confirmed and found to be caused by rapid cooling following a belt-furnace firing process. This thermal deactivation occurs independently of any subsequent permanent deactivation induced by illuminated annealing and is likely related to the dissociation of the defect and subsequent loss of defect precursors to other species. Further, by varying the surface dielectric present on the wafers during a rapid thermal process, it is demonstrated that in the absence of hydrogen in the wafer bulk, applying an illuminated annealing process does not result in any significant permanent deactivation of defects. In contrast, thermal deactivation occurs independently of the presence of hydrogen in the wafer bulk. This demonstrates that permanent deactivation via the thermal pathway and that via the illuminated annealing (regeneration) pathway occur independently of each other and have different underlying mechanisms. The implications of multiple pathways for permanent deactivation are discussed and the well-known three-state model is revisited in light of this information. A fourth state to represent the end point of thermal deactivation (State D) is proposed for more accurate modelling of BO defect kinetics.

1. Introduction

The boron-oxygen (BO) defect is a well-known defect in Czochralski (Cz) silicon and is known to cause carrier-induced degradation (CID) in such material [1]. Due to its metastability, the defect exists in at least three different states [2–4]: the annealed state (State A) that is recombination inactive, the degraded state (State B) that is recombination active, and the regenerated or passivated state (State C) that is also recombination inactive. In contrast to State A, which transitions into State B upon illumination (or carrier injection), State C is relatively stable [2,3] and does not show further degradation upon carrier injection. Permanent deactivation of the defect has therefore typically been thought of as the process of transitioning the defect from State B into State C – a process typically known as regeneration, which can occur in appropriately prepared samples [5–9] by the application of an illuminated anneal process [2,3].

However, there has been considerable debate regarding the mechanism underlying the permanent deactivation process. Firstly, there is incidental evidence that the net concentration of active BO defects is dependent on the thermal history of wafers [10–12], with the cooling rate following a rapid thermal anneal (firing) suspected to have a particularly strong influence on the defect concentration [10,12]. Importantly, changes in the defect density appear to occur immediately after the thermal process and before any illuminated annealing. In addition to this, firing conditions are also known to have a strong influence on the degree of permanent deactivation achieved during subsequent illuminated annealing [5,12,13].

Some authors have proposed that all permanent deactivation of the defect occurs due to a purely thermal process wherein the defect dissociates, and the precursors are lost to other species present in the wafer [12,14,15]. While this explains, at least qualitatively, the observed kinetics of regeneration (i.e. the transition from State B to State C) as well as the influence of firing conditions on the net defect density, there is also considerable evidence that regeneration is not a purely thermal process. In particular, the presence of hydrogen in the wafer bulk has been shown to have a significant influence on the degree [5,7,9,16–18]

* Corresponding author.
E-mail address: nnampalli@gmail.com (N. Nampalli).

http://dx.doi.org/10.1016/j.solmat.2017.06.041
Received 13 April 2017; Received in revised form 19 June 2017; Accepted 19 June 2017
Available online 29 June 2017

as well as the rate of regeneration [5,8,19]. Hence, several authors have proposed that permanent deactivation via regeneration (i.e. during illuminated annealing) occurs due to hydrogen passivation of the BO defect [7,9,20–23].

However, it is unclear if hydrogen passivation could be responsible for permanent deactivation of the defect that occurs immediately following high-temperature thermal treatments. This raises the question of whether there are in fact two independent pathways to reduce the net active BO defect density that have been conflated with one another in the literature. Further, the presence of an independent pathway suggests that for current understanding of the BO defect – the three-state model – may not be a complete description of the BO defect system.

This study aims to clarify these issues by distinguishing between the thermal reduction in active defect concentration that occurs during high-temperature processes ('thermal deactivation'), and the deactivation of fully formed defects that occurs during subsequent illuminated annealing ('regeneration'). The effects of these processes are separately quantified, and it is attempted to determine whether the mechanism underlying the two processes are related, and what role hydrogen may play in each case. Finally, the possibility of multiple independent pathways for deactivation of the BO defect is explored and its implications for the well-known three-state model for the BO defect are discussed.

2. Experimental details and methods

Symmetrical lifetime test structures were prepared using commercial grade 156 mm × 156 mm pseudo-square boron-doped Cz wafers (1.6 – 1.8 Ω cm) by alkaline texturing followed by acidic neutralisation. Wafers were subjected to an RCA clean and HF dip, then diffused at 795 °C for 25 min in a $POCl_3$ tube furnace followed by a drive-in diffusion at 885 °C for 30 min to achieve an emitter sheet resistance of 70 Ω/sq – a process known to be effective at gettering [24]. The phosphosilicate glass (PSG) and emitter thus formed were removed by etching ~2 μm from both surfaces, resulting in a wafer thickness of approximately 180 μm. This was done to ensure minimal concentrations of impurities other than B-O within the wafer bulk. The wafers were then RCA cleaned and a second, light $POCl_3$ diffusion at 780 °C for 30 min with a 20-min drive-in step was applied to achieve a sheet resistance of ~200 Ω/sq to aid in surface passivation.

The wafers were then divided into two groups and either (a) coated with silicon nitride (SiN_x:H) layers using plasma enhanced chemical vapour deposition (hydrogen-rich dielectric) at 350 °C, or (b) subjected to dry thermal oxidation at 900 °C for 6 h (hydrogen-free SiO_2 dielectric). The resulting SiN_x:H layer was 83 nm thick and had a refractive index of 2.08 at a wavelength of 633 nm [25]. The thermal oxide was 100 nm thick.

The normalised defect density (*NDD*) [26] was determined via carrier lifetime measurements performed on a Sinton Instruments WCT-120 quasi-steady-state photoconductance (QSSPC) lifetime tester. To do this, samples were annealed in the dark at 200 ± 3 °C for 10 min to obtain carrier lifetime of the samples in the 'annealed' state of the defect (τ_{DA}). Subsequently, the samples were light soaked for 48 h at 35 ± 3 °C under a halogen lamp with an intensity equivalent to 0.77 ± 0.03 suns (measured using a calibrated silicon reference cell). This was done to ensure complete degradation of carrier lifetime due to BO defects. Carrier lifetime was once again measured in the light-soaked state (τ_{LS}), with *NDD* then calculated as $(\tau_{LS}^{-1} - \tau_{DA}^{-1})$. This *NDD* is referred to as the initial *NDD* ($NDD_{initial}$), with measured carrier lifetimes referred to as $\tau_{DA,initial}$ and $\tau_{LS,initial}$ to distinguish them from later measurements.

All wafer groups were then fast-fired in a SierraTherm infrared belt furnace at varying peak firing temperatures (T_{peak}) at a belt speed of 200 in. per minute (roughly 5 m/min). In addition, wafers in Group A (SiN_x:H passivated samples) were fired one or more times (N_{fire} = 1, 2 or 3, where N_{fire} refers to the number of firing cycles). The temperature profile of firing profiles was determined using a Datapaq Q18 thermal profiler by measurements on dummy wafers prepared and fired identically to the samples in this study. The *NDD* was once again determined for all samples after firing (NDD_{fired}) using lifetime measurements following dark annealing ($\tau_{DA,fired}$) and light soaking ($\tau_{LS,fired}$) using the same procedure described earlier. Following this, some wafers were subjected to a 2-h illuminated annealing process (185 ± 2 °C, 0.80 ± 0.02 suns) to attempt to induce regeneration starting from the fully degraded state [7]. The carrier lifetime after regeneration (τ_{regen}) was then measured and the *NDD* after regeneration (NDD_{regen}) was calculated as $(\tau_{regen}^{-1} - \tau_{DA,fired}^{-1})$.

To better quantify the impact of firing and regeneration separately, it is necessary to determine the relative change in *NDD* before and after the process of interest. This relative change is further normalised via a quantity termed the fractional defect density (*FDD*) and is calculated separately for firing-induced changes (FDD_{firing}) and regeneration-induced changes (FDD_{regen}) as follows:

$$FDD_{firing} = 1 + \frac{NDD_{fired} - NDD_{initial}}{NDD_{initial}} = \frac{NDD_{fired}}{NDD_{initial}} \quad (1)$$

$$FDD_{regen} = 1 + \frac{NDD_{regen} - NDD_{fired}}{NDD_{fired}} = \frac{NDD_{regen}}{NDD_{fired}} \quad (2)$$

FDD so defined leads to a value of 1 when no change in *NDD* occurs after firing (or after regen), and leads to a value of 0 when firing (or regeneration) leads to total deactivation of the defect (i.e. when *NDD* after the process becomes zero).

Unless otherwise noted, all lifetime measurements in this study are reported at an injection level corresponding to $\Delta n = 0.1 \times N_A$, where Δn is the excess minority carrier density, and N_A is the base doping density (9.1×10^{15} cm^{-3} and 8.0×10^{15} cm^{-3} for the SiN_x:H- and SiO_2-passivated samples respectively).

3. Thermal deactivation and regeneration

This section presents the impact of surface preparation (i.e. hydrogen-rich SiN_x:H versus hydrogen-lean SiO_2) and firing conditions (peak temperature and multiple firing cycles) on the total number of BO defects. The results are discussed in the context of separate paths to permanently deactivate BO defects – a purely thermal process versus hydrogen passivation of the fully formed defect.

3.1. Deactivation during rapid firing

The impact of peak firing temperature on FDD_{firing} in Groups A (SiN_x:H passivated) and B (SiO_2 passivated) are plotted below in Fig. 1. All samples displayed similar $NDD_{initial}$ (i.e. before firing, not shown), whereas a large variation in NDD_{fired} was obtained after firing. This resulted in a reduction in FDD_{firing} for all samples and was strongly dependent on the firing conditions as seen in Fig. 1. FDD_{firing} decreased with increasing T_{peak} up to T_{peak} = 632 °C and then remained relatively constant up to T_{peak} = 735 °C. It can be seen that FDD_{firing} for both SiO_2 and SiN_x:H passivated samples follow almost identical trends with T_{peak}.

The trends in FDD_{firing} for $T_{peak} \leq 632$ °C largely agree with results from other studies, which also show a decrease in *NDD* with firing in this temperature range [11,13,27,28]. However, in some of the studies, *NDD* continues to decrease up to a set-point temperature, T_{set}, of 1050 °C before increasing again [10], whereas in others, *NDD* appears to increase with T_{set} for T_{set} higher than at least 650 °C [13]. Differences in the sample passivation and/or thermal ramp conditions could be responsible for lower *NDD* achieved after thermal treatments in such studies.

A slight rise in the level of FDD_{firing} was observed for samples fired at T_{peak} higher than 632 °C. This is attributed to the introduction of a small concentration of non-BO related CID-causing defects. Fitting of

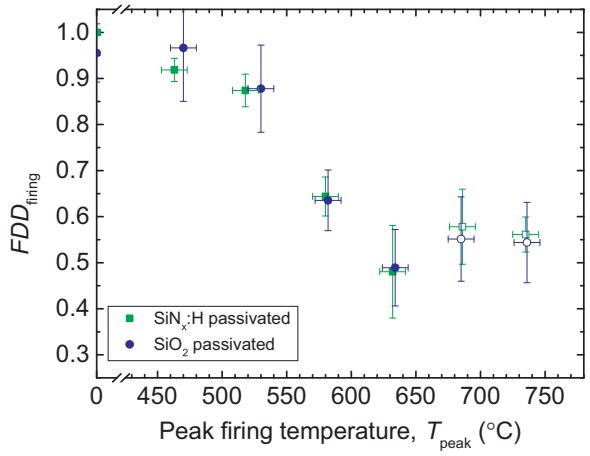

Fig. 1. FDD_{firing} for samples passivated with SiN_x:H (green squares) and SiO_2 passivation (blue circles) fired once at various T_{peak}. Firing conditions that lead to the activation of non-BO CID defects are marked (hollow data points). (For interpretation of the references to color in this figure legend, the reader is referred to the web version of this article.)

the injection-level dependent lifetime curves using the methods introduced in Ref. [29] confirmed the presence of a second SRH component in addition to BO. Further details regarding this defect will be presented in a future study; however, their impact here is minimal and thus it is assumed that they do not impact the conclusions regarding the permanent de-activation of the BO defect.

Since wafers with SiO_2 and SiN_x:H passivation are expected to introduce significantly different amounts of hydrogen into the wafer bulk during firing, this result suggests that hydrogen has no significant impact on the thermal deactivation of BO defects, which appears to be a purely thermal effect.

3.2. Impact of multiple firing steps on thermal deactivation

Further evidence that thermal deactivation due to rapid firing is a purely thermal process comes from analysis of the impact of multiple firing steps on the BO defect density. This is shown in Fig. 2 for samples with SiN_x:H surface passivation.

Importantly, there was no significant trend in FDD_{firing} with the number of firing cycles applied. This is indicated by the negligible differences between the coloured points in Fig. 2, particularly for $T_{peak} < 632$ °C.

It must be noted that increasing N_{fire} represents an increase in thermal budget at the same T_{peak}. Thus, the lack of influence of increasing N_{fire} on FDD_{firing} suggests that FDD_{firing} is independent of thermal budget. This is important for two reasons. Firstly, it makes it less likely that hydrogen passivation is involved in thermal deactivation. This is because hydrogen passivation mechanisms for bulk defects, even when they involve multiple steps, can usually be modelled by simple rate law kinetics [30], with passivation increasing with thermal budget and reducing with the loss of hydrogen [31]. This is not observed in Fig. 1 or Fig. 2 and so further supports the conclusion that hydrogen has no role in thermal deactivation.

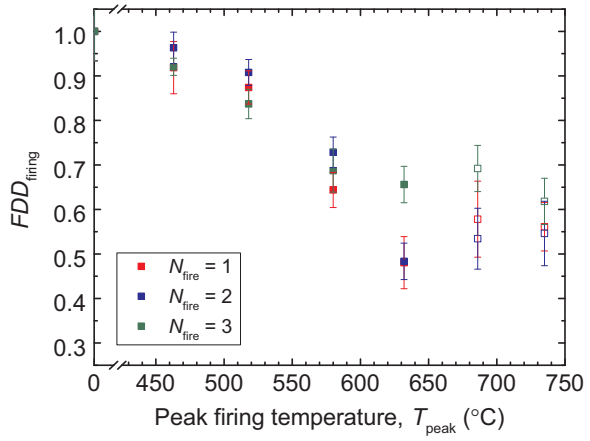

Fig. 2. Relative change in FDD_{firing} in the SiN_x:H passivated sample for firing conditions corresponding to various T_{peak} (*x*-axis) and for multiple firing cycles (colours). Hollow data points represent firing conditions where small concentrations of the non-BO CID defect are present. (For interpretation of the references to color in this figure legend, the reader is referred to the web version of this article.)

Secondly, the lack of influence of thermal budget strongly suggests that the mechanism underlying thermal deactivation is fundamentally different from that of other state transitions associated with the BO defect such as degradation, annealing, and regeneration. The typical BO-related state transitions are all known to be well modelled by simple rate law kinetics involving only a forward and reverse transition with associated Arrhenius activation energies and attempt frequencies, [4,32]. If the mechanism underlying thermal deactivation during rapid firing was also limited or governed by simple rate law kinetics it would be expected that increasing the thermal budget leads to a significant change in the final concentration of defects after the process. Since $N_{fire} = 2$ and 3 represent a doubling and tripling in thermal budget with the same T_{peak}, this should have resulted in a significant change in FDD_{firing} for wafers fired multiple times. However, this contradicts the observed data.

The idea that simple rate law kinetics are not involved is also corroborated by results from other studies that have reported that the degree of *NDD* reduction after high temperature processes such as rapid firing [12], oxidation [10,11] and diffusion [11] is significantly influenced by the cooling rates (rather than thermal budget). Proposed explanations for such behaviour in the literature typically involve complex, multi-step reactions involving dissociation of the BO defect into its precursors and freezing in of the dissociated precursors, whose concentrations are controlled by other reactions rather than by the dissociation process itself [12,14,33]. Such a mechanism can certainly explain the behaviour observed in Fig. 2.

However, it must be noted that the lack of influence from N_{fire} thermal budget would not strictly rule out more simple rate law kinetics if thermal equilibrium has already been achieved at all T_{peak} for $N_{fire} = 1$. However, in such a case, FDD_{firing} would be expected to continue reducing with increasing T_{peak} and become close to zero at sufficiently high temperatures. Since this does not appear to be the case and since the measured FDD_{firing} begins to saturate for $T_{peak} > \sim 700$ °C, it is unlikely that simple rate law kinetics are involved in thermal deactivation. A detailed comparison of the validity of the various of such models was beyond the scope of this study and will be explored in more detail in the future.

3.3. Deactivation during illuminated annealing

Note that the results presented thus far are for defect deactivation immediately after firing. The changes in *NDD* after a subsequent illuminated anneal (FDD_{regen}) are now considered for samples with various surface passivation and thermal processing, and is shown in Fig. 3 for $T_{peak} = 630$ °C. From the figure it is clear that only fired, SiN_x:H passivated samples display any substantial reduction in FDD_{regen} due to regeneration upon subsequent illuminated annealing. The lack of regeneration in hydrogen-lean samples (oxide passivated, bare and non-fired samples) confirms that hydrogen is critical for the regeneration pathway. This agrees with similar observations from other studies where wafers fired bare (i.e. without any dielectric) and non-fired wafers with and without SiN_x:H dielectrics did not undergo any regeneration [6,7]. The results from the SiO_2 passivated wafers also show that thermal deactivation occurs regardless of whether subsequent regeneration occurs. This strongly suggests that thermal deactivation and regeneration have different underlying mechanisms.

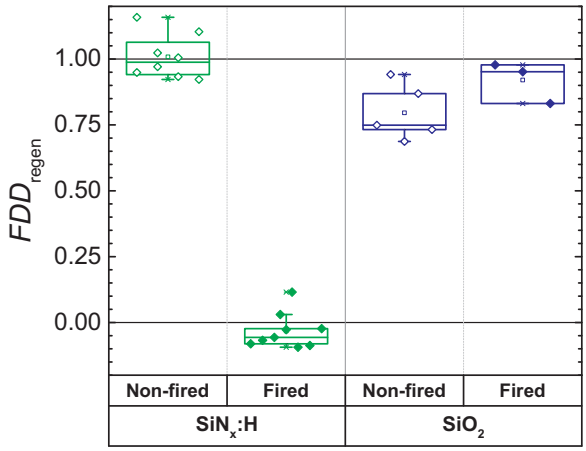

Fig. 3. Relative reduction in *NDD* after illuminated annealing (FDD_{regen}) for samples with SiN_x:H (green) and SiO_2 (blue) that were either not fired (hollow) or fired at T_{peak} = 630 °C (solid).

Other previous studies have also shown that the presence of hydrogen in the bulk is critical to induce regeneration [5,7,9,16,18,19]. This has been attributed to hydrogen passivation of the defect [20,21]; however, it has also been suggested that hydrogen does not directly passivate the BO defect but rather accelerates the rate of lifetime recovery during illuminated annealing due to improved lifetimes resulting from hydrogen passivation of background defects [8,34]. Indeed, differences in sample lifetime have been shown to induce different rates of lifetime recovery [35] due to differences in the injection levels achieved (i.e. changes in Δn) under identical illumination levels. Although kinetics of regeneration were not measured in this study, it is noted that the fired SiN_x:H- and SiO_2-passivated samples in Fig. 3 displayed similar values for carrier lifetime after firing, with almost identical values for $\tau_{LS,fired}$ (~107 μs) and comparable values for $\tau_{DA,fired}$ of ~155 μs and ~200 μs for the SiN_x:H- and SiO_2-passivated samples respectively. Hence, the difference in the degree of regeneration attributable to variations in lifetime are expected to be quite minor for the temperature and duration of the applied illuminated annealing process [35]. Since these differences do not account for the stark difference in FDD_{firing} for the two fired groups, it is concluded that regeneration is attributable mostly, if not solely, to the presence of hydrogen in the bulk.

A hydrogen-passivation model for regeneration can also explain the known behaviour of regeneration [7,21] with few contradictions thus far in the literature [8]. The main argument against the role of hydrogen has been from observations on hydrogen-lean dielectrics, particularly those deposited and processed at low temperatures (below ~200 °C) [8]. In such samples, regeneration is found to occur at extremely slow time scales, and has been presented as an argument against the involvement of hydrogen based on the low diffusivity at such temperatures of H^+, the commonly present hydrogen charge state in the dark in *p*-type silicon. However, it must be noted that hydrogen diffusion can be greatly enhanced under illumination even at such low temperatures [36] due to the formation of the fast-diffusing H° and H^-, which have orders of magnitude higher diffusivities compared to H^+. In fact, it is possible that even though there is little bulk hydrogen prior to the process, the application of an illuminated anneal could induce hydrogen diffusion in such samples, and could even limit the rate constant of regeneration [34].

While a parallel mechanism leading to regeneration (such as the action of boron nano-precipitates [12,14,15]) cannot be ruled out, hydrogen passivation of the defect appears to be the most likely mechanism for regeneration, particularly in light of the results in this work.

4. Re-evaluation of the three-state model

Based on the results presented in the previous sections, it is clear that regeneration and thermal deactivation are significantly different processes. The key points are summarised here:

- Thermal deactivation simply requires rapid cooling following a high-temperature thermal process.
- In order for regeneration to occur in a short time-scale, a firing process in the presence of a hydrogen source and subsequent illuminated anneal are required.
- There is strong reason to believe that regeneration involves hydrogen passivation of the fully formed BO defect. In contrast, thermal deactivation likely involves dissociation of the defect into its precursor states, with no apparent role of hydrogen in this process.

One important implication of multiple pathways for the permanent removal of BO defects is the impact on the stability of permanent deactivation. Hydrogen based regeneration can be destabilised to some degree by dark annealing at temperatures between 170 and 245 °C [2,21]. In particular, ~20% destabilisation has been reported to occur in a matter of 10–200 min [21], whereas near-complete destabilisation of regenerated defects appears to occur within 500 min for this range of temperatures [2]. In contrast, the destabilisation of thermally deactivated defects (i.e. thermal activation), is likely to occur at even slower timescales and at higher temperatures given the higher temperatures required to achieve thermal reduction of the BO defect concentration in the first place. However, since previous studies on destabilisation have not attempted to observe the effects of dark annealing for durations longer than 500 min, or at temperatures higher than 245 °C, the kinetics of thermal activation and its impact on the observed kinetics of destabilisation remain unknown.

Up until now, the three-state model as described by Herguth et al. [4] has been quite successful in predicting transitions between States A, B and C, which was the primary purpose of the model. Importantly, the total defect density in the three-state model, N_{tot}', which is the sum of the defect concentrations in the States A, B and C ([A], [B] and [C] respectively), is assumed to be constant in the three-state model. Since the rate of thermal activation of defects may be non-zero under certain conditions, the usual assumptions applied in the three-state model may not necessarily apply and could lead to errors in the determination of reaction kinetics.

In order to better reflect changes in N_{tot}' as well as the reaction kinetics of thermal deactivation and thermal activation, an additional state, State D, representing the state of the defect after thermal deactivation, is required to more accurately reflect the nature of the BO defect. This leads to a four-state model for the BO defect of the form shown in Fig. 4.

It must be emphasised that State D as introduced in the four-state model has a fundamentally different nature from States A, B and C. It has been demonstrated that States A and B likely involve configurational changes to the defect [37,38] rather than dissociation and formation of the defect from its precursors. Further, within a hydrogen passivation model to explain regeneration, State C is the hydrogen passivated state of the fully-formed defect. Thus, States A, B and C fundamentally refer to different configurations of a recombination centre. In contrast, State D likely represents the precursor species of the defect [33] and therefore is of a fundamentally different composition from the other states of the defect.

Further, it is proposed that State D occurs almost exclusively via a transition from State A rather than from the other states. While it could be argued that defect dissociation could occur from any of the three states, there are three main reasons why States B and C are unlikely to transition into State D. Firstly, at high temperatures (e.g. above 200 °C), State A is the preferred population at thermal equilibrium, with thermal

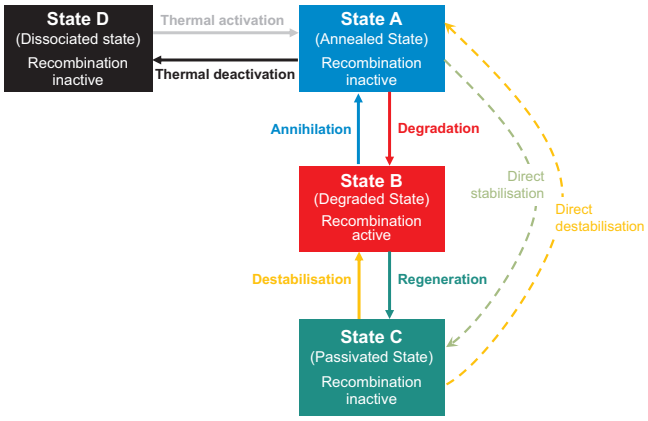

Fig. 4. Proposed four-state model for the BO defect system. States A, B and C refer to the standard states in the original model by Herguth et al. [4]. State D refers to the end state after thermal deactivation. Dashed arrows represent transitions between the defect states that have not been experimentally verified.

equilibrium achieved in a time scale of milliseconds under such conditions [39]. Thus, even when rapid thermal processing is applied, the population of States B and C may be expected to become insignificant almost immediately. Further, since State A is understood to represent a latent defect centre from which States B and C evolve [37], it is likely that State A is formed first from State D before States B and C.

Lastly, even if the transition into State D occurs from all three states, the rate constants for the transitions $B \rightarrow D$ and $C \rightarrow D$ may be expected to be in the same order of magnitude as the transition $A \rightarrow D$. Combined with the fact that State A is the preferred equilibrium population at high temperatures, the assumption that only the transition $A \rightarrow D$ applies would effectively lead to only very small predictive error if State D is indeed able to be formed from States B and C in addition to State A. Thus, the mathematical treatment of the model and the accuracy of model predictions are not expected to be significantly affected if State D is assumed to occur only from State A as opposed to being formed from all three states.

Finally, the implications of the four-state model for defect transitions and kinetic modelling are briefly discussed. An important assumption of kinetics modelling within the three-state model is that the net concentration of defects in the various states is assumed to be constant. Thus if [A], [B] and [C] refer to the concentration of defects in States A, B and C, then it is assumed that $N_{tot}' = [A](t) + [B](t) + [C](t) = \text{constant}$. However, the more correct relation is $N_{tot} = [A](t) + [B](t) + [C](t) + [D](t)$, where $N_{tot}'(t) = N_{tot} - [D](t)$. If the rate of change of [D] with time is small (i.e. thermal activation and deactivation are negligible), then $N_{tot}'(t)$ can be considered time-independent and therefore leads to the same assumption as in the three-state model.

Thus, a four-state model is not expected to impact the predictions of the three-state model under conditions where the degree of thermal activation/deactivation is insignificant. However, since thermal deactivation could occur at temperatures as low as 450 °C (or possibly even at lower temperatures at sufficiently long time scales or with sufficiently high cooling rates), failing to account for thermal activation and deactivation could introduce additional uncertainty or error in model fitting in such cases. Since time-resolved measurements were not performed in this study, the range of temperature and injection conditions where an 'effective three-state' assumption is valid could not be verified. Moreover, reaction kinetics for transitions in the three-state model have primarily been determined at temperatures lower than 450 °C, and it is unknown whether the thermal behaviour (e.g. activation energies) of such transitions can be extrapolated to higher temperatures. A detailed evaluation of thermal activation kinetics as well as the kinetics associated with the three-state model at higher temperatures will therefore be required in order to develop an accurate mathematical treatment of the four-state model. This will be the subject of future work.

5. Conclusions

In this work, permanent deactivation of BO defects via a thermal pathway and via regeneration were separately investigated on *p*-type Cz wafers fired with various surface dielectrics (no dielectric, thermal SiO_2 and PECVD SiN_x:H). The phenomenon of thermal deactivation during rapid firing was confirmed and it was shown that thermal deactivation is a fundamentally different process compared to regeneration, which occurs upon subsequent illuminated annealing. It was shown that thermal deactivation occurs even in absence of hydrogen in the wafer bulk, whereas regeneration is strongly influenced by the presence of hydrogen. This provides clear evidence that thermal deactivation and regeneration are separate pathways that both lead to permanent deactivation of the BO defect. Since the currently accepted three-state model does not account for a reduction in the total defect density due to thermal deactivation, a fourth state, State D, is proposed to account for the configuration of the BO defect after thermal deactivation. This four-state model is expected to improve the accuracy of BO kinetics modelling, particularly under conditions where thermal deactivation and thermal activation (the reverse process of thermal deactivation) are expected to dominate.

Acknowledgments

The authors would like to acknowledge Daniel Chen, Kyung Kim, Ly Mai, Nino Borojevic, and the MAiA processing team who assisted with wafer processing. This Program has been supported by the Australian Government through the Australian Renewable Energy Agency (ARENA) and the Australian Centre for Advanced Photovoltaics (ACAP). The views expressed herein are not necessarily the views of the Australian Government, and the Australian Government does not accept responsibility for any information or advice contained herein. The authors would like to thank the commercial partners of the ARENA 1-060 project, and the UK Institution of Engineering and Technology (IET) for their funding support for this work through the A.F. Harvey Engineering Prize.

References

[1] H. Fischer, W. Pschunder, Investigation of photon and thermal induced changes in silicon solar cells, in: Proceedings of the 10th IEEE Photovolt. Spec. Conference, Palo Alto, California, 1974, pp. 404–411.

[2] A. Herguth, G. Schubert, M. Kaes, G. Hahn, Avoiding boron-oxygen related degradation in highly boron doped Cz silicon, in: Proceedings 21st Eur. Photovolt. Sol. Energy Conference, Dresden, Germany, 2006, pp. 530–537.

[3] A. Herguth, G. Schubert, M. Kaes, G. Hahn, A new approach to prevent the negative impact of the metastable defect in boron doped CZ silicon solar cells, in: Proceedings of Conf. Rec. 4th World Conf. Photovolt. Energy Convers., Waikoloa, Hawaii, pp. 940–943. doi: ⟨https://dx.doi.org/10.1109/WCPEC.2006.279611⟩.

[4] A. Herguth, G. Hahn, Kinetics of the boron-oxygen related defect in theory and experiment, J. Appl. Phys. 108 (2010) 114509, http://dx.doi.org/10.1063/1.3517155.

[5] S. Wilking, A. Herguth, G. Hahn, Influence of hydrogen on the regeneration of boron-oxygen related defects in crystalline silicon, J. Appl. Phys. 113 (2013) 194503, http://dx.doi.org/10.1063/1.4804310.

[6] N. Nampalli, B. Hallam, C. Chan, M. Abbott, S. Wenham, Evidence for the role of hydrogen in the stabilization of minority carrier lifetime in boron-doped Czochralski silicon, Appl. Phys. Lett. 106 (2015) 173501, http://dx.doi.org/10.1063/1.4919385.

[7] N. Nampalli, B.J. Hallam, C.E. Chan, M.D. Abbott, S.R. Wenham, Influence of hydrogen on the mechanism of permanent passivation of boron-oxygen defects in p-Type Czochralski silicon, IEEE J. Photovolt. 5 (2015) 1580–1585, http://dx.doi.org/10.1109/JPHOTOV.2015.2466457.

[8] D.C. Walter, J. Schmidt, Impact of hydrogen on the permanent deactivation of the boron-oxygen-related recombination center in crystalline silicon, Sol. Energy Mater. Sol. Cells 158 (2016) 91–97, http://dx.doi.org/10.1016/j.solmat.2016.05.025.

[9] K. Münzer, Hydrogenated Silicon Nitride for Regeneration of Light Induced Degradation, in: Proceedings of the 24th Eur. Photovolt. Sol. Energy Conference, Hamburg, 2009, pp. 1558–1561.

[10] S.W. Glunz, S. Rein, W. Warta, J. Knobloch, W. Wettling, Degradation of carrier lifetime in Cz silicon solar cells, Sol. Energy Mater. Sol. Cells 65 (2001) 219–229,

http://dx.doi.org/10.1016/S0927-0248(00)00098-2.
[11] K. Bothe, J. Schmidt, R. Hezel, Effective reduction of the metastable defect concentration in boron-doped Czochralski silicon for solar cells, in: Proceedings of Conf. Rec. Twenty-Ninth IEEE Photovolt. Spec. Conference, IEEE, New Orleans, pp. 194–197. doi: ⟨https://dx.doi.org/10.1109/PVSC.2002.1190489⟩.
[12] D.C. Walter, B. Lim, K. Bothe, V.V. Voronkov, R. Falster, J. Schmidt, Effect of rapid thermal annealing on recombination centres in boron-doped Czochralski-grown silicon, Appl. Phys. Lett. 104 (2014) 42111, http://dx.doi.org/10.1063/1.4863674.
[13] D.C. Walter, B. Lim, K. Bothe, R. Falster, V.V. Voronkov, J. Schmidt, Lifetimes exceeding 1ms in 1-Ωcm boron-doped Cz-silicon, Sol. Energy Mater. Sol. Cells 131 (2014) 51–57, http://dx.doi.org/10.1016/j.solmat.2014.06.011.
[14] V.V. Voronkov, R. Falster, B. Lim, J. Schmidt, Permanent recovery of electron lifetime in pre-annealed silicon samples: a model based on Ostwald ripening, J. Appl. Phys. 112 (2012) 113717, http://dx.doi.org/10.1063/1.4768688.
[15] D.C. Walter, R. Falster, V.V. Voronkov, J. Schmidt, On the equilibrium concentration of boron-oxygen defects in crystalline silicon, Energy Procedia, n.d.
[16] G. Krugel, W. Wolke, J. Geilker, S. Rein, R. Preu, Impact of hydrogen concentration on the regeneration of light induced degradation, Energy Procedia 8 (2011) 47–51, http://dx.doi.org/10.1016/j.egypro.2011.06.100.
[17] P. Hamer, B. Hallam, M. Abbott, C. Chan, N. Nampalli, S. Wenham, Investigations on accelerated processes for the boron-oxygen defect in p-type Czochralski silicon, Sol. Energy Mater. Sol. Cells 145 (2016) 440–446, http://dx.doi.org/10.1016/j.solmat.2015.11.013.
[18] S. Wilking, S. Ebert, A. Herguth, G. Hahn, Influence of hydrogen effusion from hydrogenated silicon nitride layers on the regeneration of boron-oxygen related defects in crystalline silicon, J. Appl. Phys. 114 (2013) 194512, http://dx.doi.org/10.1063/1.4833243.
[19] S. Dubois, F. Tanay, J. Veirman, N. Enjalbert, J. Stendera, S. Butté, P. Pochet, D. Caliste, Y. Mao, D. Timerkaeva, D. Blanc, K. Fraser, M. Lemiti, O. Palais, I. Périchaud, B. Dridi Rezgui, V. Mong-The Yen, M. Pasquinelli, M. Gerard, F. Madon, N. Le Quang, The BOLID project: suppression of the boron-oxygen related light-induced-degradation. Presentation–main results, in: Proceedings of the 27th Eur. Photovolt. Sol. Energy Conference, Frankfurt, Germany, 2012, pp. 749–754.
[20] B.J. Hallam, S.R. Wenham, P.G. Hamer, M.D. Abbott, A. Sugianto, C.E. Chan, A.M. Wenham, M.G. Eadie, G. Xu, Hydrogen passivation of B-O defects in Czochralski silicon, Energy Procedia 38 (2013) 561–570, http://dx.doi.org/10.1016/j.egypro.2013.07.317.
[21] S. Wilking, C. Beckh, S. Ebert, A. Herguth, G. Hahn, Influence of bound hydrogen states on BO-regeneration kinetics and consequences for high-speed regeneration processes, Sol. Energy Mater. Sol. Cells 131 (2014) 2–8, http://dx.doi.org/10.1016/j.solmat.2014.06.027.
[22] M. Gläser, D. Lausch, Towards a quantitative model for BO regeneration by means of charge state control of hydrogen, Energy Procedia 77 (2015) 592–598, http://dx.doi.org/10.1016/j.egypro.2015.07.085.
[23] C. Sun, F.E. Rougieux, D. Macdonald, A unified approach to modelling the charge state of monatomic hydrogen and other defects in crystalline silicon, J. Appl. Phys. 117 (2015) 45702, http://dx.doi.org/10.1063/1.4906465.
[24] I. Périchaud, Gettering of impurities in solar silicon, Sol. Energy Mater. Sol. Cells 72 (2002) 315–326, http://dx.doi.org/10.1016/S0927-0248(01)00179-9.
[25] Z. Hameiri, N. Borojevic, L. Mai, N. Nandakumar, K. Kim, S. Winderbaum, Should the refractive index at 633 nm be used to characterize silicon nitride films?, in: Proceedings of Conf. Rec. 43rd IEEE Photovolt. Spec. Conference, IEEE, Portland, USA, pp. 2900–2904. doi: ⟨https://dx.doi.org/10.1109/PVSC.2016.7750187⟩.
[26] S. Rein, T. Rehrl, W. Warta, S.W. Glunz, G. Willeke, Electrical and thermal properties of the metastable defect in boron-doped Czochralski silicon (Cz-Si), in: Proceedings of the 17th Eur. Photovolt. Sol. Energy Conference, WIP, Munich, 2001, pp. 1555–1560.
[27] D.C. Walter, B. Lim, J. Schmidt, Realistic efficiency potential of next-generation industrial Czochralski-grown silicon solar cells after deactivation of the boron-oxygen-related defect center, Prog. Photovolt. Res. Appl. 24 (2016) 920–928, http://dx.doi.org/10.1002/pip.2731.
[28] D.C. Walter, B. Lim, K. Bothe, V.V. Voronkov, R. Falster, J. Schmidt, Effect of rapid thermal annealing on recombination centres in boron-doped Czochralski-grown silicon, Appl. Phys. Lett. 104 (2014), http://dx.doi.org/10.1063/1.4863674.
[29] N. Nampalli, T.H. Fung, S. Wenham, B. Hallam, M. Abbott, Statistical analysis of recombination properties of the boron-oxygen defect in p-type Czochralski silicon, Front. Energy 11 (2017) 4–22, http://dx.doi.org/10.1007/s11708-016-0442-6.
[30] A. Zamouche, Formation and passivation kinetics of gold-hydrogen complexes in n -type silicon, J. Appl. Phys. 93 (2003) 753–755, http://dx.doi.org/10.1063/1.1524012.
[31] E. Sveinbjörnsson, O. Engström, Reaction kinetics of hydrogen-gold complexes in silicon, Phys. Rev. B. 52 (1995) 4884–4895, http://dx.doi.org/10.1103/PhysRevB.52.4884.
[32] B. Hallam, M. Abbott, J. Bilbao, P. Hamer, N. Gorman, M. Kim, D. Chen, K. Hammerton, D. Payne, C. Chan, N. Nampalli, S. Wenham, Modelling kinetics of the boron-oxygen defect system, Energy Procedia 92 (2016) 42–51, http://dx.doi.org/10.1016/j.egypro.2016.07.008.
[33] V. Voronkov, R. Falster, The nature of boron-oxygen lifetime-degrading centres in silicon, Phys. Status Solidi 13 (2016) 712–717, http://dx.doi.org/10.1002/pssc.201600016.
[34] V. Voronkov, R. Falster, Permanent deactivation of boron-oxygen recombination centres in silicon, Phys. Status Solidi 253 (2016) 1721–1728, http://dx.doi.org/10.1002/pssb.201600082.
[35] S. Wilking, S. Ebert, C. Beckh, A. Herguth, G. Hahn, of apples and oranges: Why comparing BO regeneration rates requires injection level correction, in: Proceedings of the 32nd Eur. Photovolt. Sol. Energy Conference, Munich, Germany, 2016, pp. 487–494.
[36] D. Mathiot, Modeling of hydrogen diffusion in n- and p-type silicon, Phys. Rev. B. 40 (1989) 5867, http://dx.doi.org/10.1103/PhysRevB.40.5867.
[37] V.V. Voronkov, R. Falster, Latent complexes of interstitial boron and oxygen dimers as a reason for degradation of silicon-based solar cells, J. Appl. Phys. 107 (2010) 53509, http://dx.doi.org/10.1063/1.3309869.
[38] D. Macdonald, F. Rougieux, A. Cuevas, B. Lim, J. Schmidt, M. Di Sabatino, L.J. Geerligs, Light-induced boron-oxygen defect generation in compensated p-type Czochralski silicon, J. Appl. Phys. 105 (2009) 93704, http://dx.doi.org/10.1063/1.3121208.
[39] B.J. Hallam, M.D. Abbott, N. Nampalli, P.G. Hamer, S.R. Wenham, Implications of accelerated recombination-active defect complex formation for mitigating carrier-induced degradation in silicon, IEEE J. Photovolt. 6 (2016) 92–99, http://dx.doi.org/10.1109/JPHOTOV.2015.2494691.